J. Innovative Eng. Nat. Sci., vol. 4, no. 1, pp. 198-219, 2024.
http://doi.org/10.61112/jiens.1383887

JIENS
Journal of Innovative Engineering and Natural Science
(Yenilikçi Mühendislik ve Doğa Bilimleri Dergisi)
journal homepage: https://jiens.org
Original Paper

Determination of optimal cross-section dimensions of rectangular hollow sections under oblique bending: analytical and numerical study

Mirali Nuraliyev[a] and Mehmet Akif Dundar[a,*]

[a] *Yozgat Bozok University, College of Engineering, Mechanical Engineering Department, 66100, Yozgat/Turkey.*

ARTICLE INFO

Article history:
Received 31 Oct 2023
Received in revised form 15 Dec 2023
Accepted 10 Jan 2024

Available online

Keywords:
Optimum Design
Rectangular Hollow Section (RHS)
Rectangular Solid Section
Oblique Bending
Finite Element Analysis

ABSTRACT

An insignificant number of rigorous studies have been devoted to the development of analytical procedures that determine the optimal cross-section dimensions of rectangular hollow section (RHS) members subjected to oblique bending, despite their ubiquity in numerous application fields. In response to this, an analytical procedure has been developed based on the concept of minimizing maximum effective stress in the RHS caused by an applied oblique bending moment, in order to reduce material costs without compromising strength requirements. The RHS members addressed in this study have been assumed to be produced by hollowing out rectangular solid sections at different cross-section area extraction ratios; therefore, only the wall thicknesses of the RHS members have been taken into consideration as design variables. The minimization of maximum effective stress has been achieved by establishing a functional correlation between the cross-section design variables. The proposed procedure allows specifying the optimal cross-sectional dimensions for given different cross-section area extraction ratios and bringing cost-effective use of materials. After the subtle mathematical calculations, the derived analytical expressions have been made available to practical engineering in simple math forms for use in real design applications. The analytical procedure has been validated against numerical results which have been extracted from finite element analyses carried out in Abaqus engineering software.

I. INTRODUCTION

Since the invention of steel, hollow section members have been widely used as structural components in numerous application fields including construction and aviation due to their special features [1, 2]. The hollow sections are generally recognized for their good mechanical performance against different types of loadings such as compression, torsion, and bending in all directions [3]. Nevertheless, one of the main drawbacks of hollow sections is their higher production costs compared to other sections [3]. Thus, the ubiquity of hollow sections in many industrial application fields as well as their higher manufacturing costs make their optimal design more important for the reduction of material cost. In a robust optimal design, significant design aspects, including strength and material type, need to be taken into consideration in a balanced way [3–7].

As with other types of hollow sections, the optimal cross-section dimensions of rectangular hollow sections (RHSs) subjected to any type of load can be determined based on either adequate-strength [8–12] or adequate-stiffness [10, 13, 14]. In those two approaches, a design objective is to achieve minimum weight by determining the optimal cross-section dimensions of RHSs that satisfy strength requirements since a type of material from which a structure is manufactured, as well as its associated mechanical properties are known prior to the design. In other words, the objective function which gives the optimal cross-section dimensions and therefore minimum mass is defined in both approaches based on the satisfaction of strength requirements. Different from them, an optimal design can

*Corresponding Author: Tel: +90-544-463-4075, e-mail: m.akif.dundar@yobu.edu.tr

occasionally be required to be conducted for some specific cases where a made of material of the structure is not known before the optimal design [3, 15]. The common approach to specify the optimal dimensions of RHSs in these cases is first to minimize the maximum effective stress on the cross-section induced by applied loads, and then to select one of the most suitable materials offering higher strength than the minimized maximum effective stress. This signifies that a cost-effective design can be accomplished based on the selection of suitable materials for the production of RHSs members.

Despite high material costs brought by the wide use of the RHS members in the industry, an insignificant number of rigorous research has been devoted to specifying their optimal cross-section dimensions for the loading configuration of oblique bending to reduce their material costs [15–18]. Comparatively speaking, analytical studies which determine the optimal cross-section dimensions of RHSs for oblique bending are relatively immature compared to other loading configurations like axial compression and pure bending [17–22]. In order to fill this noticed deficiency in literature, this analytical study has been dedicated to the identification of the optimal cross-section dimensions of RHS members subjected to oblique bending.

Analytical expressions derived for the determination of the optimal cross-section dimensions of RHSs have been presented clearly and made available to practical engineering for use in actual designs. The consideration of the reported analytical expressions for the optimal design allows the cost-effective use of materials. The analytical expressions have been derived based on the idea of minimizing the maximum effective stress on the cross-section of RHSs induced by oblique bending. Since it has been assumed that the RHSs taken into consideration for the optimal design are manufactured by hollowing out the rectangular solid sections at different cross-sectional area extraction ratios, the minimization of the maximum effective stress on the cross-section has been achieved by varying the wall thicknesses of the RHSs, taking into account that the reduction ratio of the cross-sectional area remains constant. In order to give a deeper insight into the understanding of a complicated analytical procedure developed for the optimal design of RHSs, it has been applied to two different optimization problems and thus the optimal dimensions of the RHSs have been determined quantitatively.

In the first optimization problem addressed, the optimal design has been achieved based on the assumption that the material of the RHS member and its associated properties required for strength analysis are given before the design. In this case, the limit values of the angles where the oblique bending load can be applied have been first determined, and then the optimal cross-sectional dimensions have been specified accordingly.

In the second optimization problem considered, the optimal design has been performed for a given constant oblique bending angle. In this case, the optimal cross-sectional dimensions leading to the minimization of the induced maximum effective stress have been first computed with respect to the given bending angle, and then one of the most suitable materials offering higher strength than the found minimum value of the maximum effective stress has been selected.

II. DESCRIPTION OF THE OPTIMAL DESIGN PROBLEM AND THEORETICAL APPROACH

Aiming to determine the optimal cross-section dimensions of RHS members subjected to oblique bending by means of the analytical procedure that has been developed based on the aspect of the minimization of the maximum effective stress, the optimization problem of RHSs addressed in the context of this study is as described in Fig.1.

As seen in Fig.1, the RHSs have been assumed to be attained by hollowing out the rectangular solid section with the cross-section dimensions of B x H at different cross-section area extraction ratios.

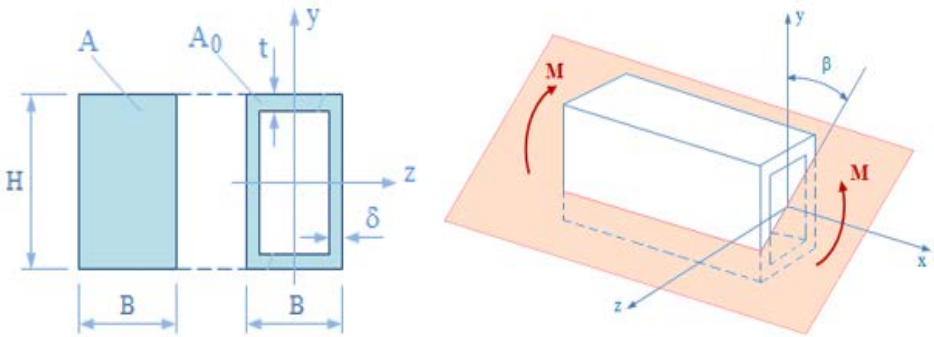

Figure 1. The optimization problem of the RHSs addressed for oblique bending

The analytical procedure has been formulated in terms of the cross-section parameters depicted in Fig.1; however, as can be understood from Fig.1, the height (H) and the width (B), of the RHS are constant and therefore not the variable design parameters. Thus, the present model consists in specifying the optimum values of the variable design parameters such as a thickness of the web (δ) and a thickness of the flange (t), as well as assessing the effect of the oblique bending moment (M) angle (β) on those two cross-section design variables.

In order to derive the analytical expressions, one of the most important conditions defined is that a reduction ratio in the cross-sectional area of the RHSs remains constant while varying the cross-section parameters of t and δ in an attempt to find their optimal values which minimize the maximum effective stress taking place on the cross-section as a result of the applied oblique bending.

The analytical approach is started with a definition of the reduction ratio for the cross-section area of the rectangular solid section, as follows:

$$\frac{\Delta A}{A} = \frac{A - A_0}{A} = c\ (constant) \tag{1}$$

where A and A_0 represent the cross-section areas of the rectangular solid section and the rectangular hollow section, respectively. Note that the defined parameter of c characterizes the reduction in the cross-section area of the rectangular solid section after hollowing it out and this parameter is given before the optimal design in order to facilitate the derivation of the analytical expressions.

The associated cross-section areas above can readily be defined in terms of the cross-section parameters, as given below.

$$A = BH \tag{2}$$

$$A_0 = BH - (B - 2\delta)(H - 2t) \tag{3}$$

As illustrated in Fig.1, B and H herein are the width and height of both the rectangular solid and hollow sections, respectively. Additionally, t and δ denote the thickness of the flange and web segments of the RHS as seen in Fig.1.

As mentioned previously, the analytical procedure has been intended to be established based on the target of minimizing the maximum effective stress on the cross-section of the RHS caused by the applied oblique bending moment in order to specify the optimal values of the cross-section parameters of t and δ for a given desired values of c. In response to this, the objective function has been described as given below. The analytical expressions required to determine the optimal values of the cross-section design variables can be derived by finding the extremums of the defined function in Eq.4.

$$\sigma_{max} = \left[\left(\frac{M_z}{I_z} y_{max} + \frac{M_y}{I_y} z_{max}\right) = \left(\frac{M cos\beta}{W_z} + \frac{M sin\beta}{W_y}\right)\right] \rightarrow \min \tag{4}$$

Herein, σ_{max} is the maximum effective stress resulting from the applied oblique bending moment (M). M_z is the z-axis component of the applied bending moment (M) axis and defined as $M_z = Mcos\beta$. In the same manner, M_y denotes the y-axis component of the bending moment (M) and is described as $M_y = Msin\beta$. Note that β is the oblique bending moment angle shown in Fig.1 Additionally, I_z and I_y are the moments of inertia about z and y axes, respectively. Furthermore, W_z and W_y are the section modulus of the RHS about the z and y axes, respectively. W_z and W_y have been derived and written as given below.

$$w_z = \frac{I_z}{y_{max}} = \frac{BH^2}{6}\left[1 - \left(1 - \frac{2\delta}{B}\right)\left(1 - \frac{2t}{H}\right)^3\right] \tag{5}$$

$$w_y = \frac{I_y}{z_{max}} = \frac{HB^2}{6}\left[1 - \left(1 - \frac{2t}{H}\right)\left(1 - \frac{2\delta}{B}\right)^3\right] \tag{6}$$

The cross-section area of the RHS(A_0) has been reformulated in terms of the section modulus, as written below.

$$A_0 = BH\left\{1 - \left[\left(1 - \frac{6w_z}{BH^2}\right)\left(1 - \frac{6w_y}{HB^2}\right)\right]^{1/4}\right\} \tag{7}$$

Taking into account Eq.7, the expression given in Eq.1 has been rearranged as given below.

$$\frac{A - A_0}{A} = \left(1 - \frac{6w_z}{BH^2}\right)\left(1 - \frac{6w_y}{HB^2}\right) - c^4 = 0 \tag{8}$$

After the subtle mathematical extractions and arrangements, the optimization problem has been brought to the determination of the optimum section modulus of the RHS with regard to the z and y axes, which meets the objective function requirement documented in Eq.4 as well as the additional design requirement described in Eq.8. Thus, the following Lagrangian objective function has been written with the help of Eq.4 and Eq.8.

$$\Phi = \left\{\frac{Mcos\beta}{W_z} + \frac{Msin\beta}{W_y} + \lambda\left[\left(1 - \frac{6w_z}{BH^2}\right)\left(1 - \frac{6w_y}{HB^2}\right) - c^4\right]\right\} \rightarrow min \tag{9}$$

where λ is the unknown Lagrange multiplier [23–25].In order to find the minimums of the function given in Eq.9, the following constraints have been defined.

$$\frac{\partial\Phi}{\partial W_z} = 0, \frac{\partial\Phi}{\partial W_y} = 0, \frac{\partial\Phi}{\partial\lambda} = 0 \tag{10}$$

The above expressions have been represented by the set of equations given below.

$$\begin{cases} \dfrac{\partial\Phi}{\partial W_z} = -\dfrac{Mcos\beta}{w_z^2} + \lambda\left[\left(-\dfrac{6}{BH^2}\right)\left(1 - \dfrac{6w_y}{HB^2}\right)\right] = 0 \\ \dfrac{\partial\Phi}{\partial W_y} = -\dfrac{Msin\beta}{w_y^2} + \lambda\left[\left(-\dfrac{6}{HB^2}\right)\left(1 - \dfrac{6w_z}{BH^2}\right)\right] = 0 \\ \dfrac{\partial\Phi}{\partial\lambda} = \left(1 - \dfrac{6w_z}{BH^2}\right)\left(1 - \dfrac{6w_y}{HB^2}\right) - c^4 = 0 \end{cases} \tag{11}$$

By solving the set of equations above together, the analytical expressions that give the optimum moment resistances of the RHS (W_z , W_y) have been derived as written below.

$$w_z = \frac{(1-c^4)B^2H^2}{6\left(B + c^2\sqrt{BH\tan\beta}\right)} \tag{12}$$

$$w_y = \frac{(1-c^4)B^2H^2}{6\left(H + c^2\sqrt{BH\cot\beta}\right)} \tag{13}$$

The analytical expressions to determine the variable cross-section parameters of δ and t which satisfy the optimum moment resistances of W_z and W_y have been finally obtained as written below after solving Eq.5 and Eq.12 together as well as solving Eq.6 and Eq.13 simultaneously.

$$t = \frac{H}{2}\left[1 - \sqrt[8]{\frac{(BH^2 - 6w_z)^3}{BH^5\left(HB^2 - 6w_y\right)}}\right] \tag{14}$$

$$\delta = \frac{B}{2}\left[1 - \sqrt[8]{\frac{(HB^2 - 6w_y)^3}{HB^5(BH^2 - 6w_z)}}\right] \tag{15}$$

For a given design problem example (M = 25 kN.m, H = 200 mm, B= 100 mm and c = 0.8), the effects of the oblique bending angle (β) on the important parameters of t, δ and σ_{max} have been assessed accounting for Eq.4 and Eqs.(12-15) in order to give a closer look at the proposed procedure. The calculated results are tabulated in Table.1.

Table 1. The effects of the various oblique bending moment angles on the parameters of t,δ and σ_{max}

β, Degree	W_z, mm^3	W_y, mm^3	t, mm	δ, mm	σ_{max}, MPa
0	393600	0	28.45	-5.90	63.50
10	285205	94719	15.43	2.70	132.20
20	254585	112449	12.10	4.49	168.30
30	233213	123340	9.85	5.63	194.20
40	215189	131724	8.00	6.52	211.00
45.75	205318	136037	7.00	7.00	216.60
50	197981	139126	6.26	7.33	218.80
53.50	191796	141655	5.64	7.61	219.40
60	179630	146444	4.44	8.14	217.40
70	157425	154593	2.28	9.10	206.30
80	124737	165374	-0.80	10.32	183.70
90	0	196800	-11.80	14.22	127.00

As clearly seen in Fig.2, the web thickness of the RHS (δ) becomes equal to the flange thickness of the RHS (t) at a unique oblique bending moment angle designated β_0. As can be deduced from Fig.2, if the angle of the oblique bending moment with the vertical of the plane (β) on which the moment, M, is applied is less than β_0, the flange thickness is larger than the web thickness ($t > \delta$). If the opposite is the case ($\beta > \beta_0$), the flange thickness is less than the web thickness ($t < \delta$).

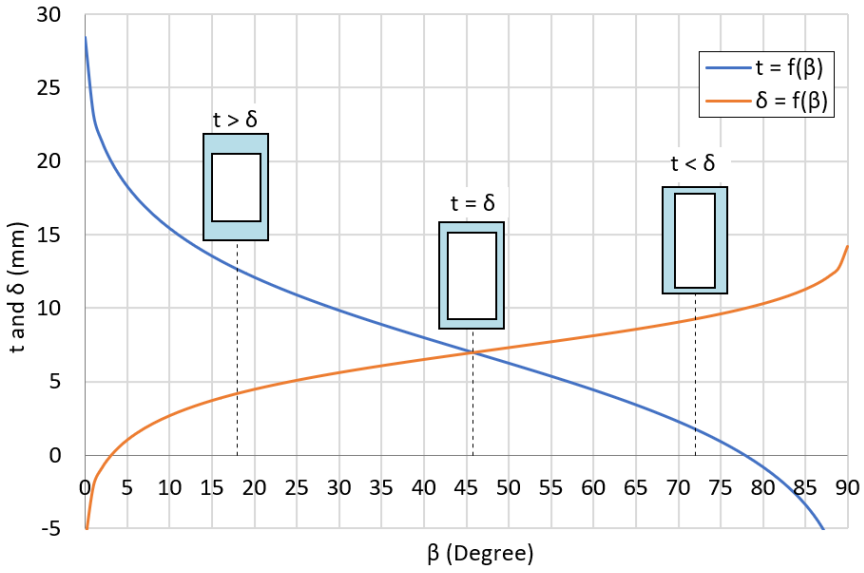

Figure 2. The effect of oblique bending moment angle on t and δ, ($t = f(\beta)$ and $\delta = f(\beta)$).

At this specific angle where the web thickness is identical to the flange thickness, the relevant segment thicknesses of the RHS, designated t_0 and δ_0, corresponding to this unique angle can be obtained using the following derived expression.

$$t_0 = \delta_0 = \frac{1}{4}\left[(H+B) - \sqrt{(H+B)^2 - 4HB(1-c)}\right] \tag{16}$$

The analytical expression giving the specific bending moment angle of β_0 which defines the wall thicknesses of the RHS has been derived by accounting for the equality of Eq.14 to Eq.15, as given below.

$$\beta_0 = \tan^{-1}\left[\frac{1}{c^4 H/B}\left(1 - \frac{1-c^4}{1-ck^2}\right)^2\right] \tag{17}$$

where k is the notation and described as follows:

$$k = \frac{1}{2}\left[1 - \frac{B}{H}\left(1 - \sqrt{\left(1 + \frac{H}{B}\right)^2 - 4(1-c)\frac{H}{B}}\right)\right] \tag{18}$$

Taking into account Eq.12 and Eq.13, as well as accounting for Eq.14 and Eq.15, the objective function given in Eq.4 has been redefined for its extremum, as written below.

$$\sigma_{max} = \frac{6M}{(1-c^4)H^2B^2}\left(H\sin\beta + B\cos\beta + c^2\sqrt{2HB\sin 2\beta}\right) \tag{19}$$

For the given design problem (M = 25 kNm, H = 200 mm, B = 100 mm, c = 0.8), the unknown parameters have been calculated to be $t_0 = \delta_0$ = 7.0 mm, β_0 = 45.750 and σ_{max}= 216.6 MPa. Note that these quantitatively obtained results with the exception of σ_{max} actually confirm the previously reported outcomes in Fig.2.

In the light of all the information presented above, the optimum design steps are summarized for the convenience of the designers, as follows;

In the first step, the optimum values of the design variables, t and δ, are extracted from Eq.14 and Eq.15, respectively.

In the second step, the extremum value of maximum effective stress, σ_{max}, is determined by using Eq.19.

In the third step, a cost-effective material selection for the production of the RHS is carried out based on the design requirement of $\sigma_y/S > \sigma_{max}$.

Herein, σ_y represents the yield strength of the selected material and S is regarded as the factor of safety. The material qualities of the selected materials need to satisfy the defined strength requirement of $\sigma_y/S > \sigma_{max}$ for robust design.

As seen in Table 1, increasing the oblique bending moment angle, β, from 0˚to 50˚ leads to an improvement in the extremum value of the maximum normal stress. On the contrary, altering the angle of β from 500 to 900 results in a decrease in the extremum value of the maximum normal stress. This actually signifies that there is a transition point where the maximum normal stress goes from increasing to decreasing. The oblique bending moment angle designated β_k, corresponding to this transition point can be determined by means of the derived formula given below. Note that the following expression has been attained by taking into account Eq.19.

$$\left.\frac{\partial\sigma_{max}}{\partial\beta}\right|_{\beta=\beta_k} = 0 \;\Rightarrow H\cos\beta_k - B\sin\beta_k + c^2\cos 2\beta_k\sqrt{\frac{2HB}{\sin 2\beta_k}} = 0 \tag{20}$$

For the addressed design problem, the transition point angle, β_k, has been found to be 53.5°, in addition, the corresponding maximum stress, σ_{max} , has been computed to be 219.4 MPa. Based on this finding, it has been concluded that it is recommended to avoid not only the angle of β_k but also its immediate vicinity to impose the oblique bending moment on the RHS unless there are no additional requirements specified (technological, structural, etc.). This suggestion is made based on the finding that the highest normal stress takes place on the RHS at β_k. Thus, a high-strength material selection is required for the production of the RHS, which cannot be considered the right choice from an economic point of view.

Table 2 shows the optimum quantitative results of the cross-section design variables computed for different cross-sectional area extraction ratios of c by using the expressions given in Eq.12-Eq.15 and Eq.19.

Table 2. The computed cross-section design variables for different values of c

Cross-sectional area extraction ratio, c	**Optimum cross-section parameters**				**Maximum normal stress**
	w_z, mm^3	**w_y, mm^3**	**t, mm**	**δ, mm**	**σ_{max}, MPa**
	M= 25.10^6 N.mm, β = 30^0, H = 200 mm, B = 100 mm				
0.40	554299	282706	35.10	19.19	83.28
0.50	492653	253519	27.75	15.40	93.25
0.60	418408	217325	21.22	11.92	109.26
0.70	331862	173970	15.30	8.68	137.10
0.80	233213	123340	9.85	5.63	194.18
0.90	122576	65363	4.77	2.74	367.87

In contrast to the previously addressed design problem, if a production material of the RHS and therefore its associated mechanical properties are known prior to optimal design, the cross-section variables of δ and t are defined after determining the limit values of the angle, β, to which the oblique bending moment, M, is applied. In this case, the determination of the limits of the bending moment angle, β, can be achieved by using the following expression, which has been obtained by redefining the objective function given in Eq.4 for the relation of $\sigma_{max} = \frac{\sigma_y}{S}$.

$$\sigma_{max} = \frac{\sigma_y}{S} \Rightarrow \frac{6M}{(1-c^4)H^2B^2}\left(H\sin\beta + B\cos\beta + c^2\sqrt{2HB\sin 2\beta}\right) = \frac{\sigma_y}{S} \tag{21}$$

To give a deeper understanding of what the extremums of the objective function, reported for the different values of c in Table 2, signify, the objective function (Eq.4) has been first rewritten as a function of t and δ , and then the graphical representation of the related extremums has been attained by using the newly defined functions given below.

$$\sigma_{max}(t) = \frac{6M\cos\beta}{BH^2[1-c(1-2t/H)^2]} + \frac{6M\sin\beta(1-2t/H)^2}{HB^2[(1-2t/H)^2-c^3]} \tag{22}$$

$$\sigma_{max}(\delta) = \frac{6M\sin\beta}{HB^2[1-c(1-2\delta/B)^2]} + \frac{6M\cos\beta\,(1-2\delta/B)^2}{BH^2[(1-2\delta/B)^2-c^3]} \tag{23}$$

Additionally, the expression defining the parameter of δ in terms of t has been obtained as given below.

$$\delta(t) = \frac{B}{2}\left(1-\frac{c}{1-2t/H}\right) \tag{24}$$

In essence, graphical representations which provide a profound summary of the associated data tabulated in Table 2 have been obtained by accounting for Eq.22, Eq.23 and Eq.24 and presented for some of the various values of c in Fig.3.

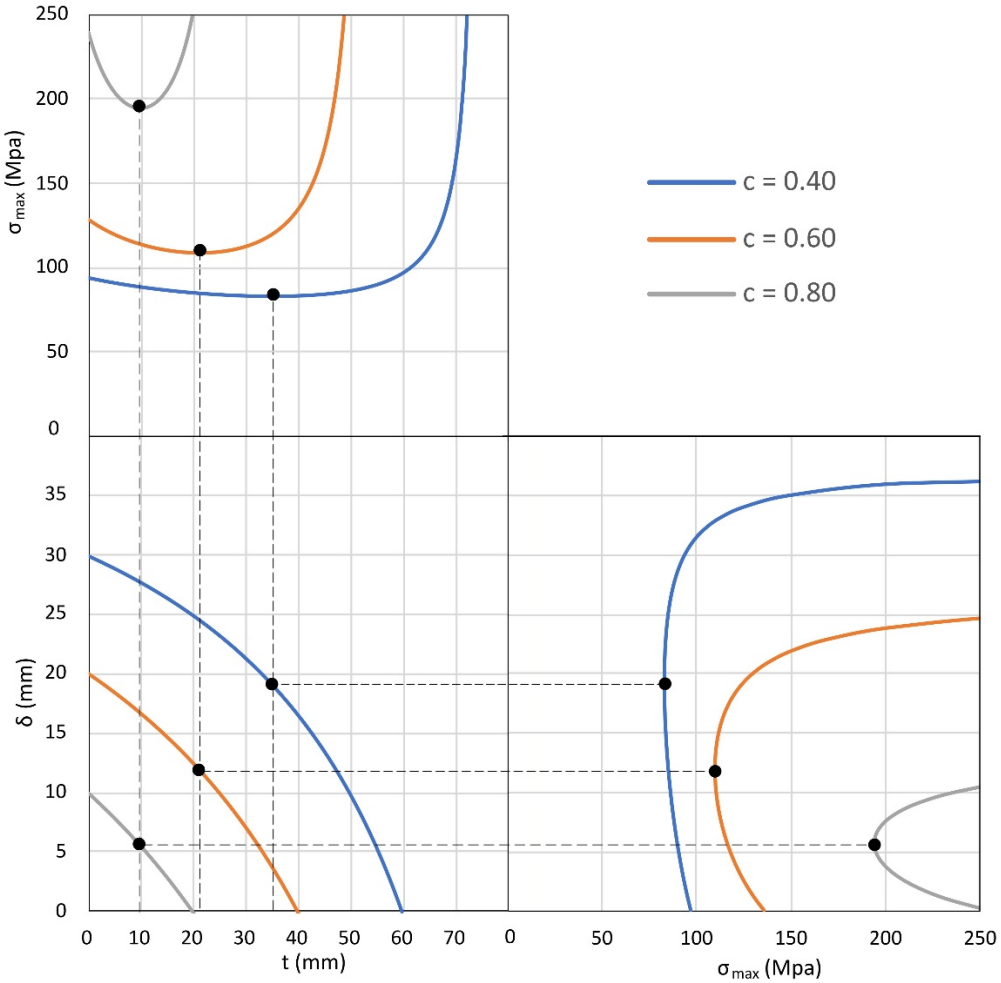

Figure 3. Graphs of $\delta = f(t)$, $\sigma_{max} = f(t)$ and $\sigma_{max} = f(\delta)$ attained for some of the different values of c

III. OPTIMUM DESIGN EXAMPLES WITH THE DEVELOPED ANALYTICAL PROCEDURE

This section presents the detailed solutions of the two distinct optimal design problems which shed light on the developed procedure for a better understating of its application steps. The first problem addressed is the design problem in which the production material of the RHS is obvious and the yield strength of this material is known before the optimal design. Opposite to the first problem, the second problem handled is the case where a lack of information on the manufacturing material of the RHS exists but the oblique bending moment angle is given.

The RHS taken into consideration in both optimal design problems has been assumed to be attained by hollowing out the rectangular solid section with a dimension of 200x100 mm ($h \times b$ = 200×100 mm) at the cross-section extraction ratio of 0.8 (c=0.8). Additionally, the RHS has been presumed to be subjected to the oblique bending moment of 25 kN.m (M=25 kN.m).

An application of the derived analytical expressions to the first addressed optimal design problem of finding the optimal dimensions of the RHSs is as follows:

In this case, allowable stress that can be taken in the RHS has been given as 162 MPa (σ_y/S = 162 MPa) prior to the optimal design. Additionally, the RHS taken into consideration for the optimum design is assumed to be produced from Grade-250 medium-strength steel that is widely utilized as load-carrying components in structural applications. The elastic and plastic material properties of Grade-250 steel are found in the literature as; mean elastic modulus E = 209 GPa, Poisson's ratio ν = 0.3, and mean yield strength σ_{yield} = 290 MPa [26, 27].

Since the oblique bending moment angle (β) is not known, the calculations begin with the determination of the limit values that the oblique bending moment angle (β) can take. This has been achieved by substituting the applied moment of 25 kN.m and allowable stress of 162 MPa into Eq.20, as a result of this, the limit values of β have been found to be 18° and 86°. The variation of the maximum normal stress (σ_{max}) with the oblique bending moment angle (β) is graphically presented in Fig.4. The limit values for the oblique bending moment angle can also be readily extracted from Fig.4. The presented results in Fig.4 are actually a graphical representation of the results obtained by using Eq.17.

Of these two limit values, only the angle of 18° has been taken into account and accordingly, the section modulus(w_z, w_y) and cross-section design variables (t, δ) have been computed as follows:

$$w_z = \frac{(1-c^4)B^2H^2}{6\left(B + c^2\sqrt{BH\tan\beta}\right)} = \frac{(1-0.8^4)100^2 \cdot 200^2}{6\left(100 + 0.8^2\sqrt{100 \cdot 200 \cdot \tan 18^0}\right)} = 259644 \text{ mm}^3$$

$$w_y = \frac{(1-c^4)B^2H^2}{6\left(H + c^2\sqrt{BH\cot\beta}\right)} = \frac{(1-0.8^4)100^2 \cdot 200^2}{6\left(200 + 0.8^2\sqrt{100 \cdot 200 \cdot \cot 18^0}\right)} = 109704 \text{ mm}^3$$

$$t = \frac{H}{2}\left[1 - \sqrt[8]{\frac{(BH^2 - 6w_z)^3}{BH^5(HB^2 - 6w_y)}}\right] = \frac{200}{2}\left[1 - \sqrt[8]{\frac{(100 \cdot 200^2 - 6 \cdot 259644)^3}{100 \cdot 200^5(200 \cdot 100^2 - 6 \cdot 109704)}}\right] = 12.64 \text{ mm}$$

$$\delta = \frac{B}{2}\left[1 - \sqrt[8]{\frac{(HB^2 - 6w_y)^3}{HB^5(BH^2 - 6w_z)}}\right] = \frac{100}{2}\left[1 - \sqrt[8]{\frac{(200 \cdot 100^2 - 6 \cdot 109704)^3}{200 \cdot 100^5(100 \cdot 200^2 - 6 \cdot 259644)}}\right] = 4.21 \text{ mm}$$

Maximum normal stress taken place in the RHS has been found to be 162 MPa, as given below.

$$\sigma_{max} = \frac{M\cos\beta}{W_z} + \frac{M\sin\beta}{W_y} = \frac{25{\cdot}10^6{\cdot}\cos 18^0}{259644} + \frac{25{\cdot}10^6{\cdot}\sin 18^0}{109704} = 162 \text{ MPa} = \frac{\sigma_y}{S}$$

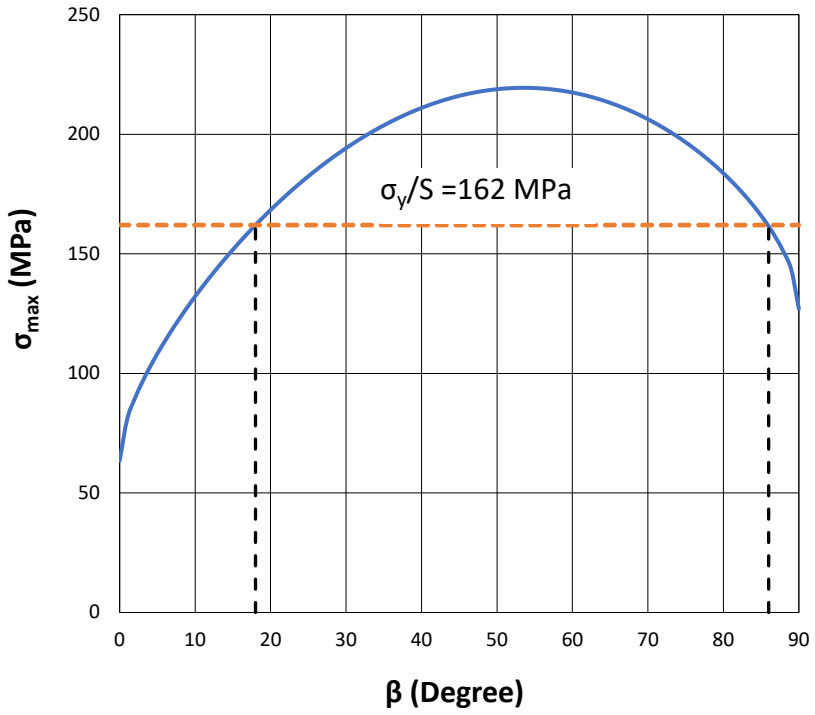

Figure 4. The variation of maximum normal stress with oblique bending moment angle of β

Note that the identical result for maximum normal stress above can also be obtained by using Eq.19 that has been previously derived to identify the extremums of maximum normal stress. By using Eq.19, maximum normal stress has been calculated as given below.

$$\sigma_{max} = \frac{6M}{(1-c^4)H^2B^2}\left(H\sin\beta + B\cos\beta + c^2\sqrt{2HB\sin 2\beta}\right) = \frac{6{\cdot}25{\cdot}10^6}{(1-0.8^4){\cdot}200^2{\cdot}100^2}\left(200 \cdot \sin 18^0 + 100 \cdot \cos 18^0 + 0.8^2\sqrt{2 \cdot 200 \cdot 100 \cdot \sin(2 \cdot 18^0)}\right) = 162 \text{ MPa}.$$

The second optimal design problem dealt with is the case in which the oblique bending moment angle is constant and equal to β = 30°. Thus, the following calculations are associated with the solution of the referred problem.

First, the optimum section modulus of the RHS about z and y axes have been determined for β = 30° by using Eq.12 and Eq.13, respectively, as follows:

$$w_z = \frac{(1-c^4)B^2H^2}{6\left(B+c^2\sqrt{BH\tan\beta}\right)} = \frac{(1-0.8^4)100^2\cdot200^2}{6\left(100+0.8^2\sqrt{100\cdot200\cdot\tan30^0}\right)} = 233213 \text{ mm}^3$$

$$w_y = \frac{(1-c^4)B^2H^2}{6\left(H+c^2\sqrt{BH\cot\beta}\right)} = \frac{(1-0.8^4)100^2\cdot200^2}{6\left(200+0.8^2\sqrt{100\cdot200\cdot\cot30^0}\right)} = 123340 \text{ mm}^3$$

Second, the optimum design variables of t and δ have been specified by means of Eq.14 and Eq.15, respectively, as given below.

$$t = \frac{H}{2}\left[1-\sqrt[8]{\frac{(BH^2-6w_z)^3}{BH^5\left(HB^2-6w_y\right)}}\right] = \frac{200}{2}\left[1-\sqrt[8]{\frac{(100\cdot200^2-6\cdot233213)^3}{100\cdot200^5(200\cdot100^2-6\cdot123340)}}\right] = 9.85 \text{ mm}$$

$$\delta = \frac{B}{2}\left[1-\sqrt[8]{\frac{(HB^2-6w_y)^3}{HB^5(BH^2-6w_z)}}\right] = \frac{100}{2}\left[1-\sqrt[8]{\frac{(200\cdot100^2-6\cdot123340)^3}{200\cdot100^5(100\cdot200^2-6\cdot233213)}}\right] = 5.63 \text{ mm}$$

Third, in order to make sure of the section modulus-related calculations above, the determined optimum values of w_z and w_y have been verified using both Eq.5 and Eq.6 which have been previously derived for the determination of the section modulus of the RHS, as given below.

$$w_z = \frac{BH^2}{6}\left[1-\left(1-\frac{2\delta}{B}\right)\left(1-\frac{2t}{H}\right)^3\right] = \frac{100\cdot200^2}{6}\left[1-\left(1-\frac{2\cdot5.63}{100}\right)\left(1-\frac{2\cdot9.85}{200}\right)^3\right] = 233230\ mm^3$$

$$w_y = \frac{HB^2}{6}\left[1-\left(1-\frac{2t}{H}\right)\left(1-\frac{2\delta}{B}\right)^3\right] = \frac{200\cdot100^2}{6}\left[1-\left(1-\frac{2\cdot9.85}{200}\right)\left(1-\frac{2\cdot5.63}{100}\right)^3\right] = 123341\ mm^3$$

Finally, the maximum normal stress occurring in the cross-section of the RHS has been found as follows:

$$\sigma_{max} = \frac{M\cos\beta}{W_z} + \frac{M\sin\beta}{W_y} = \frac{25{\cdot}10^6{\cdot}\cos 30^0}{233230} + \frac{25{\cdot}10^6{\cdot}\sin 30^0}{123341} = 194.17 \text{ MPa}$$

The maximum normal stress has been further calculated by using Eq.19 to validate the above result, as given below.

$$\sigma_{max} = \frac{6M}{(1-c^4)H^2B^2}\left(H\sin\beta + B\cos\beta + c^2\sqrt{2HB\sin 2\beta}\right) = \frac{6{\cdot}25{\cdot}10^6}{(1-0.8^4){\cdot}200^2{\cdot}100^2}\left(200\cdot \sin 30^0 + 100\cdot\cos 30^0 + 0.8^2\sqrt{2\cdot 200\cdot 100\cdot\sin(2\cdot 30^0)}\right) = 194.18 \text{ MPa.}$$

Based on the determined maximum normal stress of 194.18 MPa, a designer is suggested to select one of the most suitable materials with a higher yield strength than 194.18 MPa for a robust and cost-effective design.

As a summary of this section, two distinct optimal design problems have been solved by applying the derived analytical expressions to the problems step by step. The analytical expressions, which have been derived and well-documented for use in the optimal design of the RHSs subjected to oblique bending, can be easily used by any designer who encounters similar design cases in industrial applications.

IV. FINITE ELEMENT MODELING

Aiming to validate the obtained analytical results, finite element analyses have been implemented on the RHS subjected to oblique bending using the finite element code of Abaqus. The grid geometries of the RHSs have been meshed using the incompatible mode eight-node brick elements, designated C3D8I [28]. Using this element type in such numerical implementations in which linear elements are subject to bending is highly recommended for high accuracy [28]. Particularly, the C3D8I element removes shear locking as well as significantly reducing volumetric locking [28]. The geometric nonlinearity option in Abaqus has been activated during the numerical analyses because of the nonlinear geometry of the RHSs. The finite element model of the RHS under oblique bending including the imposed boundary conditions and bending moments is depicted in Fig.5. The elastic and plastic mechanical properties of the RHS material given below [26, 27] have been successfully introduced to the finite element model to predict the deformation behavior of the RHS subject to the oblique bending moment.

E=209000 MPa, ν = 0.3, and σ_{yield} = 290 MPa.

The boundary conditions and bending moments have been applied to the reference points defined at the geometric center of both ends, as shown in Fig.5. These imposed boundary conditions and loads have been transferred from the reference points to the RHS via the defined kinematic couplings [4, 29]. After studying a mesh convergence, an average number of elements of 55680 corresponding to a number of nodes of 70795 have been decided to use

in the numerical implementations. The result of the mesh convergence study obtained for the RHS with equal wall thicknesses (δ=t=7 mm) subject to the oblique bending moment applied at $\beta = 45.75^{\circ}$ is illustrated in Fig. 9. As comprehended from the results presented in Fig.9, the numerical results start to converge when the finite element model comprises 52800 elements with an average size of 2.23. Therefore, this mesh convergence study has given a concrete idea of whether the solution converged or not [30, 31].

The numerical analyses have been first performed to verify the analytical results reported in Section 3. After the validation of the results given in Section 3, the finite element analysis has also been carried out to validate the analytical results for some of the oblique bending moment angles documented in Table 1, in order to be completely sure that the analytical results are validated.

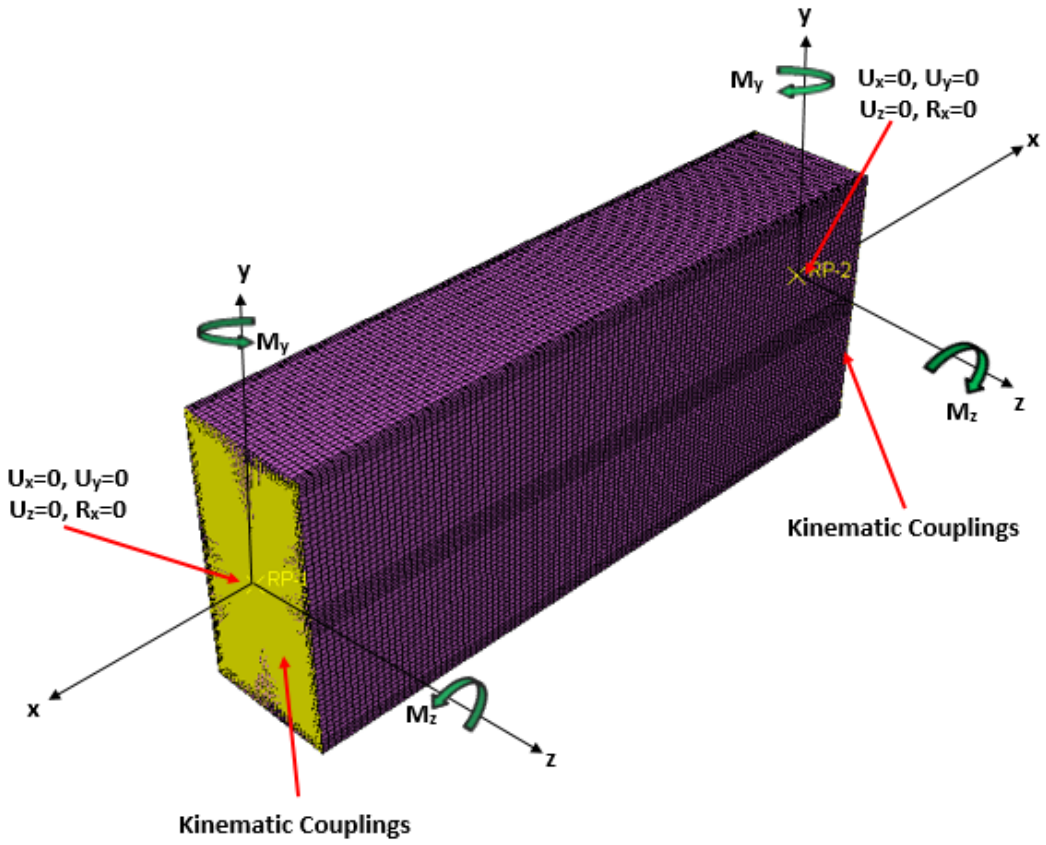

Figure 5. The finite element model of the RHS under oblique bending

V. RESULTS AND VALIDATION

The numerically obtained effective stress contour of the RHS subjected to an oblique bending moment at the angle of 18^{0} is depicted in Fig. 6. Previously, the maximum effective stress for this case has been analytically found to be 162 MPa. As can be seen in Fig.6, the maximum effective stress extracted from the numerical analysis has also been found to be 162 MPa, implying that the analytical results are in an identical agreement with the numerical prediction.

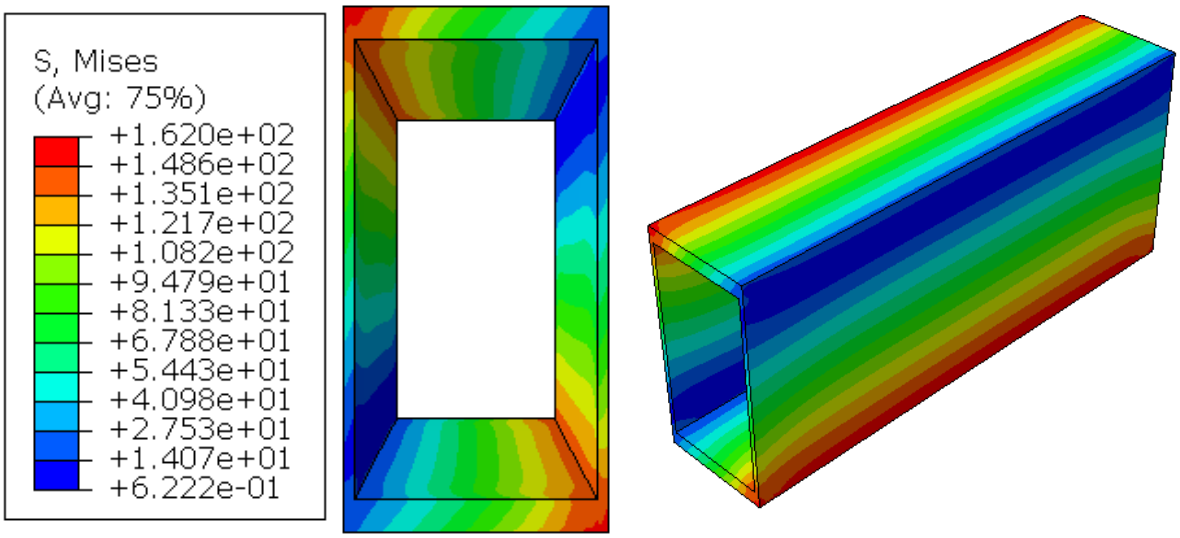

Figure 6. Maximum effective stress contour of the RHS under oblique bending ($t = 12.64\ mm, \delta = 4.21\ mm, and\ \beta = 18^0$), (a) Cross-sectional view, (b) Isometric view

Previously, the ranges of angles to which the oblique bending moment of M is allowed to be applied have been determined to be (0° – 18°) and (86° - 90°), as depicted in Fig.4. Nevertheless, the ranges of angles of (0° – 3°) and (78° - 90°) are not the viable ranges to which the oblique bending moment can be applied since the flange thickness takes a negative value in the range of (0° – 3°) as well as the web thickness in the range of (78° - 90°). Therefore, the oblique bending simulation has been performed for the angle of 18°. As seen in Fig.4, the RHS subjected to oblique bending in the interval of $18^\circ < \beta < 86^\circ$ does not meet the defined strength requirement of $\frac{\sigma_y}{S}$ = 162 MPa since maximum bending stresses occurring in the RHS are higher than the allowable stress of 162 MPa in this interval.

Fig.7 shows the effective stress contour of the RHS imposed to an oblique bending moment at the angle of 30°. The maximum effective stress has been predicted to be 194.4 MPa, as seen in Fig.7. For this optimal design problem, the maximum effective stress has been calculated to be 194.17 MPa using the derived expressions earlier. Thus, a very insignificant error ratio of 0.14% has been found between the numerical predictions and analytical calculations.

By means of the above simulations, the analytical solutions of the optimum design problems documented under Section 3 have been verified. Additional simulations have been performed to predict the oblique bending response of the RHS for some of the different angles given in Table 1, in order to make sure of the verification of the developed analytical procedure.

As can be seen in Fig.7 and Fig.8, the maximum effective stress takes place in the upper left and lower right corners of the RHS. The stress distribution in the RHS resulting from the oblique bending moment has been determined by several researchers [32–34]. It has been seen that the stress distribution in the RHS (Fig.7, and Fig. 8) extracted from the numerical analyses is in good agreement with the results reported by those studies [32–34].

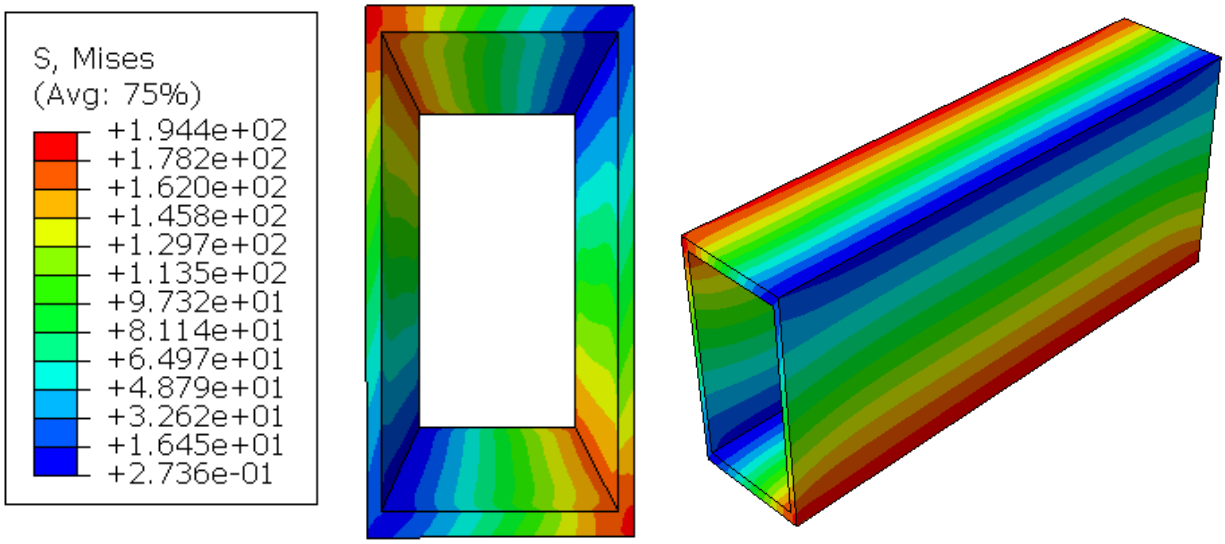

Figure 7. Maximum effective stress contour of the RHS under oblique bending (t=9.85 mm,δ=5.63 mm, and β= 30˚), (a) Cross-sectional view, (b) Isometric view

The effective stress contours of the RHS subjected to oblique bending at various moment angles ranging from 10˚ to 70˚ are illustrated in Fig.8. In terms of the maximum effective stress, the numerically predicted results are favorably compared to the analytical results as shown in Fig.10.

As deduced from both Fig.2 and Fig.8, increasing the oblique bending moment angle (β) leads to a decrease in the flange thickness of RHS (t) but an increase in the web thickness of RHS (δ). This can be mainly due to the following reasons.

According to the angle of the applied moment, the graphics presented in Fig.2 can be divided into four distinct regions including $0^\circ \leq \beta < 3^{0^\circ}$, $3^\circ \leq \beta \leq 45.75^\circ$, $45.75^\circ < \beta < 78^\circ$ and $78^\circ \leq \beta \leq 90^\circ$.

In the region where the angle ranges from 0˚ to 3˚, the optimum cross-section parameter of δ takes negative values signifying that this angle range is not feasible to apply the oblique bending moment.

In the angle range from 3˚ to 45.75˚, the optimum flange thickness of the RHS is always larger than the optimum web thickness($t > \delta$). This is because, since $M_z > M_y$ in this range, the optimum resistance required for major and minor axis bending is mostly met by the flange segments [35]. In addition, it should be noted that the flange and web thicknesses are equal to 20 mm and 0 mm, respectively when $\beta = 3^\circ$. This actually implies that the RHS consists of only the flange segments at this angle $\beta = 3^\circ$. In this case, the optimum resistance required for major and minor axis bending is completely compensated by the flange segments since the moment of M_z is much larger than the moment of M_y ($M_z \gg M_y$) [32, 36, 37].

Furthermore, the flange thickness becomes equal to the web thickness ($\delta = t = 7$) when the β reaches its value of 45.75° ($M_z \cong M_y$). This suggests that the deformation mechanism of the RHS under oblique bending is equally controlled by both segments [32, 36, 37]

Bending Moment Angle, β, Degree	Cross-Sectional View	Isometric View
10^0	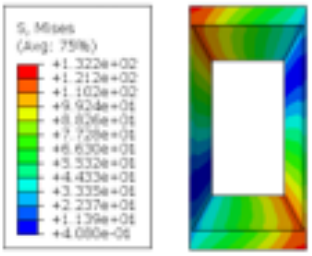 $t = 15.13\ mm$ $\delta = 2.7\ mm$	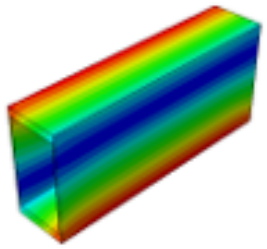
45.75^0	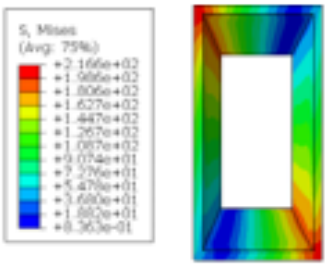 $t = 7\ mm$ $\delta = 7\ mm$	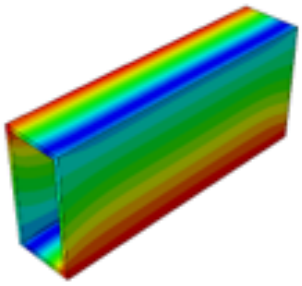
53.5^0	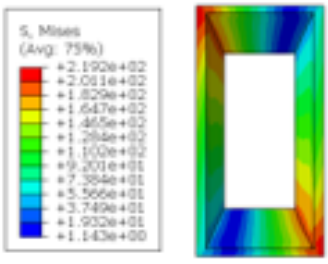 $t = 5.64\ mm$ $\delta = 7.61\ mm$	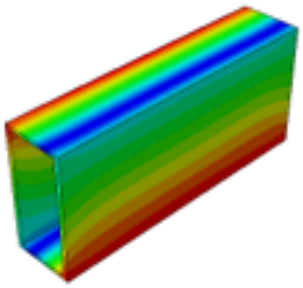
60^0	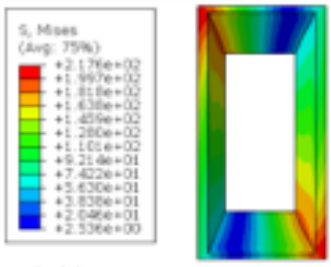 $t = 4.44\ mm$ $\delta = 8.14\ mm$	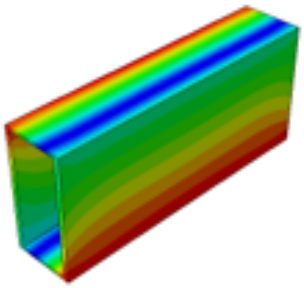
70^0	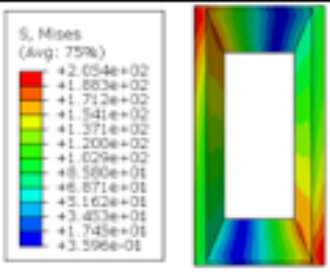 $t = 2.28\ mm$ $\delta = 9.1\ mm$	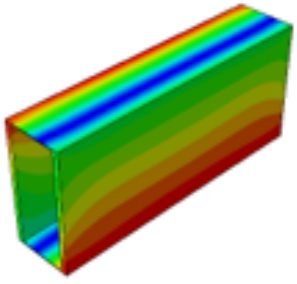

Figure 8. Effective stress contours of the RHS under oblique bending with different moment angles

In the angle range from 45.75° to 78°, the RHS is under M_y-dominated bending which results in a higher thickness in the web than the flange. In other words, the flange thickness is always less than the web thickness in this region. The web segments play a primary role in providing the optimum resistance to major and minor axis bending.

In the region where the angle ranges from 78° to 90°, the flange takes negative thickness values as illustrated in Fig.2, which indicates that applying the oblique bending moment in this angle range is not practicable for optimum design. Besides this, the flange and web thickness at $\beta = 78^{\circ}$ are equal to 0 and 10 mm, respectively($t = 0$ and $\delta = 10mm$). At this angle of 78°, the flange segments of the RHS begin to vanish, pointing out that the RHS comprises only the web segments. In essence, the deformation mechanism of the RHS is totally controlled by the web segments when $M_y \gg M_z$ [32, 36, 37]

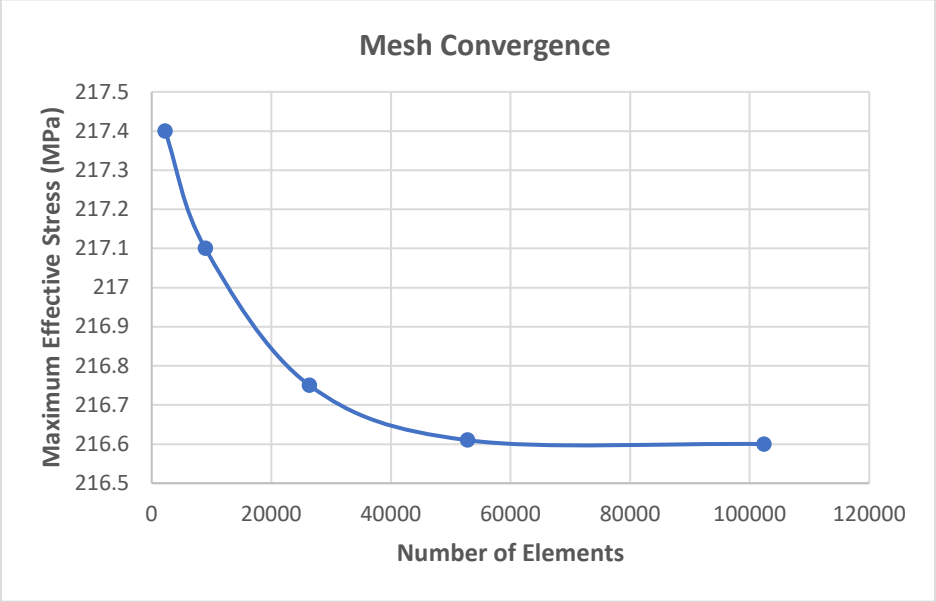

Figure 9. The result of the mesh convergence study obtained for the RHS with equal wall thicknesses ($\delta = t = 7\ mm$) subject to the oblique bending moment applied at $\beta = 45.75^{0}$

The result of the mesh convergence study obtained for the RHS with an identical wall segment thickness ($\delta = t = 7\ mm$) subjected to the oblique bending moment imposed at $\beta = 45.75^{\circ}$ is illustrated in Fig.9. It is clearly seen in Fig. 9 how the simulation results converge with the number of elements used in the numerical analysis. The number of elements used in finite elements plays an important role in calculation accuracy. Therefore, it is imperative to determine how many elements should be used in the simulations by performing a mesh convergence study.

As illustrated in Fig.10, accomplishing a very good agreement between the analytical and numerical results confirms the developed analytical procedure, and therefore the analytical expressions derived in the context of this study.

Nevertheless, the numerical results insignificantly deviate from the theoretical results as the oblique bending moment angle β increases, as seen in Fig.10. At the β=70°, the discrepancy between the numerical and theoretical results becomes slightly obvious. As noted before, as the oblique bending moment angle β increases, the

component of the oblique bending moment of the y-axis (M_y) enhances, while its component about the z-axis (M_z) decreases. These two moment components are equal at β=45˚, in addition, M_y is always larger than M_z for the values of β larger than 45˚. This signifies that the web segments of the RHS become more prone to bending with increasing oblique bending moment angle. The reason for the insignificant inconsistency found between the numerical and analytical results may be that the side walls become more susceptible to bending due to the increasing angle.

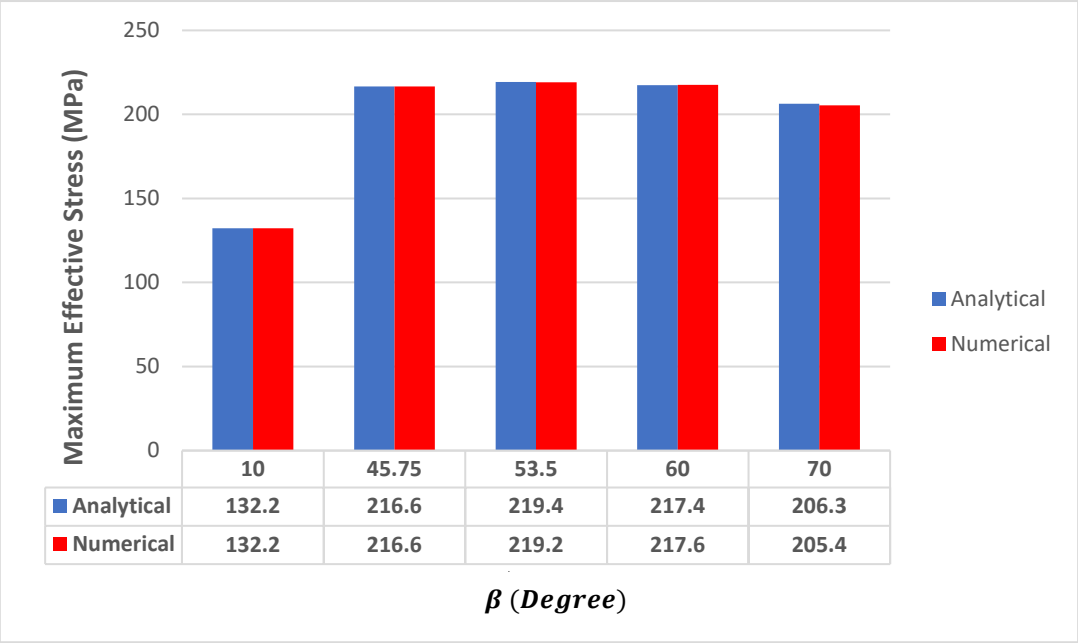

	10	45.75	53.5	60	70
Analytical	132.2	216.6	219.4	217.4	206.3
Numerical	132.2	216.6	219.2	217.6	205.4

Figure 10. The comparison of the analytical maximum effective stress with the numerical predictions for different oblique bending moment angles

VI. CONCLUDING REMARKS

The following conclusions have been drawn from the findings of this study.

The analytical expressions which define the optimum cross-section dimensions of the RHS subjected to oblique bending moment have been derived and successfully applied to the two distinct optimal design problems. The analytical procedure has been developed based on the aspect of minimizing the maximum effective stress on the cross-section of RHS caused by the applied oblique bending moment. Since the RHSs addressed in this study have been assumed to be produced by hollowing out the rectangular solid sections at different cross-section area extraction ratios, the analytical procedure allows specifying the optimal cross-section dimensions for different cross-section area subtraction ratios.

After the subtle mathematical calculations, the derived analytical expressions have been made available to practical engineering in a simple and understandable math form for use in real design applications.

The cost-effective design can be achieved following the steps of the analytical procedure for two distinct optimal design cases.

If a manufacturing material of the RHS is known prior to the design, the analytical procedure first defines the limit values of the oblique bending moment angle and then, based on this, minimizes the maximum effective stress by finding the optimum values of the cross-section design variables.

If a production material of the RHS is not known but the oblique bending moment angle is given before the design, the analytical procedure optimizes the cross-section variables to minimize the maximum effective stress by taking into account the given bending moment angle. In this optimal design case, one of the most cost-effective materials offering a higher yield strength than the found maximum effective stress can be selected from a relevant table. The application steps of the derived analytical expressions to these two different design problems have been well documented under Section 3, in order to give a deep insight into the analytical procedure. By following the analytical procedure steps presented in Section 3, the optimal design can be achieved by any designer who encounters one of the two aforementioned problems.

The analytical procedure has been validated against the numerical results that have been extracted from the finite element analysis carried out in Abaqus engineering software.

In essence, the analytical procedure developed within the scope of this study has helped paved the way to meet the need for analytical procedures related to this field.

REFERENCES

[1] Chavan V, Nimbalkar V, Jaiswal A (2007) Economic Evaluation of Open and Hollow Structural Sections in Industrial Trusses. Int J Innov Res Sci Eng Technol 3297:2319–8753
[2] Mendoza JMG, Montes SA, Lomelí JJ, Campos JAF (2017) Size optimization of rectangular cross section members subject to fatigue constraints. J Theor Appl Mech 55:547–557
[3] Wardenier J, Packer JA, Zhao X-L, Van der Vegte GJ (2002) Hollow sections in structural applications. Bouwen met staal Rotterdam,, The Netherlands
[4] Dundar MA, Nuraliyev M, Sahin DE (2022) Determination of Optimal Dimensions of Polymer-Based Rectangular Hollow Sections Based on Both Adequate-Strength and Local Buckling Criteria: Analytical and Numerical Study. Mech Based Des Struct Mach. https://doi.org/10.1080/15397734.2022.2139720
[5] Shigley JE, Mitchell LD, Saunders H (1985) Mechanical engineering design
[6] Wardenier J, Dutta D, Yeomans N (1995) Design guide for structural hollow sections in mechanical applications. Verlag TÜV Rheinland
[7] Weaver PM, Ashby MF (1996) The Optimal Selection of Material and Section-shape. J Eng Des 7(2):129–150. https://doi.org/10.1080/09544829608907932
[8] Deshpande VS, Fleck NA (2001) Collapse of truss core sandwich beams in 3-point bending. Int J Solids Struct 38(36):6275–6305. https://doi.org/https://doi.org/10.1016/S0020-7683(01)00103-2
[9] Wicks N, Hutchinson JW (2001) Optimal truss plates. Int J Solids Struct 38(30):5165–5183. https://doi.org/https://doi.org/10.1016/S0020-7683(00)00315-2
[10] Ashby M, Evans A, Fleck N, Gibson L, Hutchinson J, Wadley HNG (2002) Metal Foams: a Design Guide. Mater Des 23:119. https://doi.org/10.1016/S0261-3069(01)00049-8
[11] Zok FW, Rathbun HJ, Wei Z, Evans AG (2003) Design of metallic textile core sandwich panels. Int J Solids Struct 40(21):5707–5722. https://doi.org/https://doi.org/10.1016/S0020-7683(03)00375-5
[12] Wadley HNG, Fleck NA, Evans AG (2003) Fabrication and structural performance of periodic cellular metal sandwich structures. Compos Sci Technol 63(16):2331–2343. https://doi.org/https://doi.org/10.1016/S0266-3538(03)00266-5
[13] Zenkert D (1995) An Introduction to Sandwich Construction. Engineering Materials Advisory Services
[14] Gibson LJ (2003) Cellular Solids. MRS Bull 28(4):270–274. https://doi.org/DOI: 10.1557/mrs2003.79
[15] Ivanovich SA (2016) Оптимальные размеры прямоугольного сечения бруса при косом изгибе. Вестник евразийской науки 8(2 (33)):134
[16] Wang W, Qiu X (2018) Analysis of the Carrying Capacity for Tubes Under Oblique Loading. J Appl Mech 85(3). https://doi.org/10.1115/1.4038921
[17] Chen DH, Masuda K (2015) Estimation of Collapse Load for Thin-Walled Rectangular Tubes Under Bending.

J Appl Mech 83(3). https://doi.org/10.1115/1.4032159
[18] Paulsen F, Welo T (2001) Cross-sectional deformations of rectangular hollow sections in bending: Part II — analytical models. Int J Mech Sci 43(1):131–152. https://doi.org/https://doi.org/10.1016/S0020-7403(99)00107-1
[19] Su R, Tangaramvong S, Van TH (2023) An BESO Approach for Optimal Retrofit Design of Steel Rectangular-Hollow-Section Columns Supporting Crane Loads. Buildings 13(2):328
[20] Kuhn J, Packer JA, Fan Y (2019) Rectangular hollow section webs under transverse compression. Can J Civ Eng 46(9):810–827
[21] Bedair O (2015) Novel design procedures for rectangular hollow steel sections subject to compression and major and minor axis bending. Pract Period Struct Des Constr 20(4):4014051
[22] Rincón-Dávila D, Alcalá E, Martín Á (2022) Theoretical–experimental study of the bending behavior of thin-walled rectangular tubes. Thin-Walled Struct 173:109009. https://doi.org/https://doi.org/10.1016/j.tws.2022.109009
[23] Bertsekas DP (2014) Constrained optimization and Lagrange multiplier methods. Academic press
[24] Kannan BK, Kramer SN (1994) An augmented Lagrange multiplier based method for mixed integer discrete continuous optimization and its applications to mechanical design
[25] Ito K, Kunisch K (2008) Lagrange multiplier approach to variational problems and applications. SIAM
[26] Erasmus LA, Smaill JS (1990) The Mechanical Properties of BHP Structural Sections. Trans Inst Prof Eng New Zeal Civ Eng Sect 17(1):19–25
[27] Mahendran M (1996) The modulus of elasticity of steel-is it 200 gpa?
[28] Dassault Systèmes (2012) Abaqus Analysis User's Manual 6.12. Documentation
[29] Sellittoa A, Borrelli R, Caputo F, Riccio A, Scaramuzzino F (2011) Methodological approaches for kinematic coupling of non-matching finite element meshes. Procedia Eng 10:421–426
[30] Zhao W, Ji S (2019) Mesh convergence behavior and the effect of element integration of a human head injury model. Ann Biomed Eng 47:475–486
[31] Tso C-F, Molitoris DP, Snow S (2012) Propped cantilever mesh convergence study using hexahedral elements. Packag Transp Storage Secur Radioact Mater 23(10–2):30–35
[32] Gardner L, Fieber A, Macorini L (2019) Formulae for Calculating Elastic Local Buckling Stresses of Full Structural Cross-sections. Structures 17:2–20. https://doi.org/https://doi.org/10.1016/j.istruc.2019.01.012
[33] Vieira L (2018) On the local buckling of RHS members under axial force and biaxial bending. Thin-Walled Struct 129:10–19. https://doi.org/10.1016/j.tws.2018.03.022
[34] Shen H-X (2019) A new simple method for the strength of high-strength steel thin-walled box columns subjected to axial force and biaxial end moments. Adv Civ Eng 2019
[35] Razzaq Z, McVinnie WW (1982) Rectangular tubular steel columns loaded biaxially. J Struct Mech 10(4):475–493
[36] Bock M, Theofanous M, Dirar S, Lipitkas N (2021) Aluminium SHS and RHS subjected to biaxial bending: Experimental testing, modelling and design recommendations. Eng Struct 227:111468
[37] Zhao O, Rossi B, Gardner L, Young B (2015) Behaviour of structural stainless steel cross-sections under combined loading–Part II: Numerical modelling and design approach. Eng Struct 89:247–259